JOURNAL OF APPLIED ELECTROCHEMISTRY **27** (1997) 558–567

Sodium hydroxide and hydrochloric acid generation from sodium chloride and rock salt by electro-electrodialysis

S. MAZROU, H. KERDJOUDJ, A. T. CHÉRIF

Institut de Chimie, USTHB Dar El Beïda, Alger, Algeria

J.MOLÉNAT*

Laboratoire des Matériaux et Procédés Membranaires, CNRS BP5051, 34033 Montpellier Cedex 01, France

Received 1 June 1995; revised 23 September 1996

An electro-electrodialysis process (EED) is used to generate HCl and NaOH from trade NaCl. The key phenomenon limiting the current efficiency of this process is proton leakage through the anion selective membrane. Two new low proton leakage membranes: the ARA and ACM were used. NaOH and HCl solutions with purity higher than 99.9% are obtained. The experimental values of the fluxes for HCl and NaOH are compared with values calculated from integration of the Nernst–Planck electrodiffusion equations. This calculation requires several experimentally determined parameters: ionic diffusion coefficients, membrane conductance and amount of sorbed electrolyte. Algerian rock salt from El Outaya is used to compare electro-electrodialysis and electrodialysis using bipolar membranes.

List of symbols

$\bar{c}_S$	concentration of sorbed electrolyte
d	membrane thickness
K	constant
$\overline{n}^+$ and $\overline{n}^-$	amounts of cation and anion equivalents per fixed site
$\overline{n}_S$	amount of sorbed moles per site
z_i	electric charge of ith ion
$\overline{D}_i$	diffusion coefficient in the membrane
E_D	diffusion potential
f	$= zF/RT$
F	Faraday constant
$\overline{\Phi}$	membrane potential
I	current density
J_i	flux of ith ion
Λ	conductance in the membrane
Q	amount of electricity (coulomb)
R	perfect gas constant
R_M	membrane resistance
S	active surface of the membrane
T	absolute temperature
$\overline{U}^+$ and $\overline{U}^-$	cation and anion conventional mobilities inside the membrane
$\left[\overline{X}^+\right]$	exchange capacity of the membrane considered as concentration per unit volume

1. Introduction

Sodium hydroxide is produced from sodium chloride by several types of electrolysis: diaphragm, mercury cathode and membrane cell processes [1–3]. The purpose of this work is to use the electro-electrodialysis (EED) [4] in order to obtain NaOH and HCl instead of NaOH and Cl_2 as with the above techniques.

Electro-electrodialysis process can be performed with different types of cell. Generally EED cells consist of two, three or four compartments separated by anion exchange membranes (AEM) or cation exchange membranes (CEM). In the present case to produce sodium hydroxide and hydrochloric acid from NaCl solutions a four compartment cell was used (Fig. 1). EED is an electro-membrane technique which is easy to utilize and non polluting. Compartments are separated by ion exchange polymer membranes and the electrodes are chemically passive.

The most important phenomenon limiting the current efficiency is proton leakage [5] through the AEM membranes. Newly available AEM (ARA and ACM) low proton leakage membranes [6, 7] were used during the present experiments. This work concerns the following three membranes: (i) ARA 17/10 (an AEM manufactured by Morgane, France); (ii) ACM Neosepta (an AEM manufactured by Tokuyama Soda, Japan); and (iii) CMV Selemion (a CEM manufactured by Asahi Glass, Japan).

Because of the low selectivity of the usual anion exchange or anion selective membranes due to proton leakage, electro-electrodialysis has rarely been used in industry for acid and base production. In this work new anion selective membranes with very low proton leakage are used. In order to compare the performance of these membranes with previous ones the following electrochemical arrangement was used:

* To whom correspondence should be sent.

Table 1. Sulfate transfer number for different anion exchange membranes

AEM	*Neosepta AFN*	*Permion 4035*	*Morgane ADP5*	*Ionac MA 3475*	*Morgane ADP5*	*Neosepta ACM*	*Morgane ARA*
Θ	–0.27	–0.07	0.08	0.24	0.26	0.4	0.55

$$(-) \quad 0.5\,\text{M}\ H_2SO_4|\text{AEM}|2\,\text{M}\ H_2SO_4 \quad (+)$$

The transfer number, θ, of sulfate ion was determined for different AEM. (see Table 1). The current density was $0.04\,\text{A cm}^{-2}$ and the time of electro–electrodialysis was 30 min. With the highest values for $\theta_{SO_4^{2-}}$ the lowest values of θ_{H^+} were obtained and, consequently, the lowest proton leakage [7].

In this work the main objective was to study the influence of physicochemical parameters (nature of anion selective membrane, initial concentration, current density, sorption and current efficiency) on acid and base production.

Natural rock salt from El Outaya near Biskra in southern Algeria was used to compare EED, in which protons and hydroxide ions are generated on the electrodes, and electrodialysis (ED) with a bipolar membrane, in which the same ions are generated from water splitting [8–10].

2. Experimental details

2.1. *Electro-electrodialysis cell*

To produce HCl and NaOH simultaneously the cell was composed of four compartments separated by anion and cation exchange membranes alternatively (Fig. 1). The four compartments were filled with different solutions: sodium hydroxide in compartment I, sodium chloride in compartment II, hydrochloric acid in compartment III and sulfuric acid in compartment IV. The initial volumes were 100 mL except in compartment II which contained 250 mL of NaCl. In each compartment the solution flow was $3.6\,\text{dm}^{-3}\,\text{h}^{-1}$. The sulfuric acid concentration remained at 0.1 M in compartment IV. Experiments were performed from different initial concentrations in the three other compartments.

Compartment IV enables oxidation of chloride ions from compartment II to be avoided. Sulfuric acid was selected because sulfate ions do not react at the electrodes. A low 0.1 M H_2SO_4 concentration avoids acid diffusion from compartment IV to compartment III. On the other hand no noticeable volume variation was detected in the four compartments.

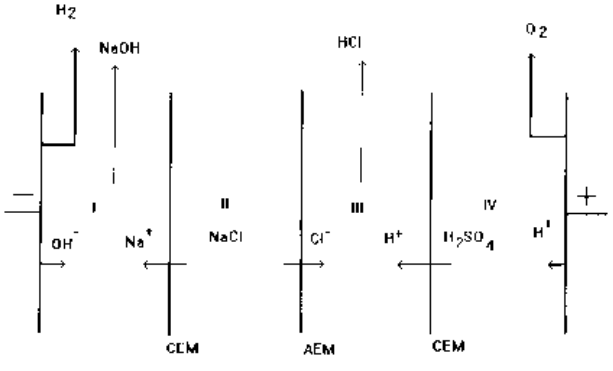

Fig. 1. The four compartment electro-electrodialysis cell to produce HCl and NaOH.

Solution flow was produced using Watson–Marlow peristaltic pumps. A beaker, used as a reservoir, was included in the loop of each compartment. Constant current was provided by a Fontaine stabilized d.c. generator. Current and voltage were measured using a multimeter.

The polymethacrylate EED cell consisted of two electrode compartments separated by two other compartments. The active area of the membrane separating the compartments was $12.5\,\text{cm}^2$. Silicone gaskets between compartments prevented leakage. The intermembrane distance was 10 mm. The platinized titanium electrodes had an area of $20\,\text{cm}^2$.

Laboratory reagent grade NaCl, HCl and NaOH were used with El Outaya NaCl rock salt, which is a natural salt of high purity. This natural rock salt was dissolved in water and then filtered before introduction to the cell. Concentration variations were followed by various titration methods. HCl and NaOH by acid–base titration, Na^+, K^+, Ca^{2+}, Mg^{2+} by spectrophotometry, SO_4^{2-} by turbidimetry and Cl^- by $AgNO_3$ titration.

From the NaCl solution (compartment II) Na^+ cations migrate through the cation exchange membrane (CEM) to the catholyte compartment to form sodium hydroxyde solution with hydroxide ions coming from water reduction at the cathode (Compartment I).

Protons from water oxidation on the anode transfer through the CEM and enter compartment III to generate hydrochloric acid with chloride ions coming from the NaCl, solution through the (AEM). Consequently, the HCl and NaOH concentrations increase as NaCl decreases.

The average current efficiency C_{eff} for compartments I and III, devoted respectively to HCl and NaOH generation, was calculated by means of the equation:

$$C_{\text{eff}} = \frac{\Delta MF}{Q} \qquad (1)$$

where ΔM is the increasing amount of moles in compartments I or III.

2.2. *Electrodialysis cell with bipolar membrane*

The six compartments of the electrodialysis cell with a bipolar membrane (BPM) (Fig. 2) were filled with different solutions at different initial concentrations: 0.2 M NaCl in compartment I, 1 M NaCl in compartment II, 0.1 M HCl in compartment III, 0.1 M NaOH

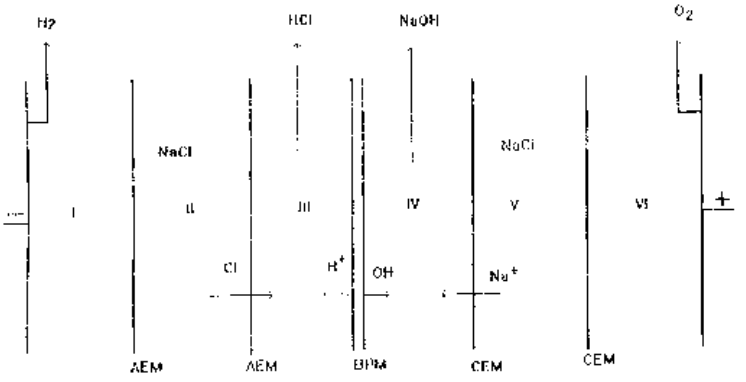

Fig. 2. The six compartment electrodialyser with BPM.

in compartment IV, 1 M NaCl in compartment V and 0.2 M Na_2SO_4 in compartment VI to avoid chloride oxidation. The initial volume was 0.800 dm^{-3} in compartments I and VI, 0.250 dm^{-3} in compartments II and V and 0.100 dm^{-3} in compartments III and IV in which acid and base concentrations were increasing. In each compartment the solution flow was 3.6 $dm^{-3}\,h^{-1}$. We used the same d.c. generator, the same cells and hydrodynamic conditions as previously. In Fig. 2, ARA and CMV are the anion and cation exchange membranes, respectively.

2.3. *Membrane stabilization*

Before using the membranes, they were submitted to a pretreatment for conditioning. The membranes were immersed in 1 M HCl and rinsed in bidistilled water. After rinsing the CEM was immersed for 1 h in 1 M NaOH and rinsed. Then the two membranes were immersed in 0.1 M NaCl. This cycle was repeated twice.

2.4. *Exchange capacity and thickness measurements*

The exchange capacities were determined by acid–base titration [11]. Table 2 gives the dry membrane weights, densities, exchange capacities and thickness of the three membranes (ARA, ACM and CMV). The membrane thickness was carefully determined with a micrometer, the membrane being placed between two parallel glass slides. The value of the membrane thickness was obtained by subtracting the values measured with and without the membrane. This technique allowed measurement of the average thickness (d) of the membrane with good accuracy, an important factor in the determination of the flux of ions or of the membrane potential.

Table 2. Weight of dry membranes, densities, exchange capacities and thickness of the utilized membranes

Membrane	*ARA*	*ACM*	*CMV*
Dry membrane weights of the used samples / g	0.2345	0.1006	0.1052
Density / g cm^{-3}	1.66	0.93	0.83
Exchange capacity / mmol cm^{-3}	0.996	0.93	1.992
Thickness / μm	157	120	140

2.5. *Determination of the sorbed HCl, NaOH and NaCl quantities in AEM and CEM*

The AEM equilibrated with Cl^- counter-ions was immersed 24 h in HCl at different concentrations. After removal from the equilibrating solution, the membrane was dried using blotting paper and immersed in stirred bidistilled water for 24 h [12]. The amount of sorbed chlorides was divided by the number of fixed sites for comparison purpose with the other membranes. The same process was used with the CEM which was equilibrated with Na^+ counter-ions by immersing in NaOH solutions. The AEM chloride desorbed quantities in water were determined using $AgNO_3$ titrations. The Na^+ desorbed quantities from the CEM were determined by flame spectrophotometry. The same process was used, with NaCl 0.5 M in which the AEM and CEM membranes were immersed for 24 h.

2.6. *Resistance measurements*

After 24 h conditioning in solution, the electric resistance was measured at 25 °C using a CD60 Tacussel conductimeter and a clip cell at 1000 Hz. The membrane was placed between two volumes of solution which separated the two electrodes from the membrane. The area of the platinized platinum disc electrodes and of the measured membrane was 1 cm^2. The resistance of the membrane was taken as the difference between the measurements with and without the membrane [13].

3. Results and discussion

3.1. *Performance of the anion exchange membranes*

The performance of the two anion exchange membranes (ARA and ACM) can be compared in Table 3 which gives the results of an experiment performed for 120 min at a current density of 120 mA cm^{-2}. Using initial solutions of 0.5 M NaCl, 0.1M HCl and 0.1 M NaOH, a final concentration of about 0.9 M was obtained with the ARA and 0.8 M with the ACM. The ARA membrane showed a lower proton leakage than the ACM. Because these experiments are time dependent, after only one hour lower concentrations but higher current efficiencies are

Table 3. Electro-electrodialysis experimental results after 120 min experiment at $I = 120\,mA\,cm^{-2}$ with 0.1 M initial concentration for HCl and NaOH

AEM	*ARA*	*ACM*
NaOH / M	0.84	0.75
Current efficiency / %	66	58
HCl / M	0.94	0.8
Current efficiency / %	75	62.5
Average voltage / V	34	24

obtained. Table 3 shows that in spite of a lower current efficiency, the ACM membrane gives a significant decrease in voltage requirement and, hence, energy demand.

3.2. *Influence of initial HCl and NaOH concentrations*

The experiments were performed for 120 min at a current density of $40\,mA\,cm^{-2}$ using initial concentrations of 0.1, 0.5, 1 and 1.5 M for HCl and NaOH and 0.5 M for NaCl.

Figures 3(a) and (b) show, for the ARA and the ACM membranes, respectively, the decreasing average current efficiency when initial acid and base concentrations increase. For HCl the obtained straight lines are in agreement with the linearly decreasing values of the transfer numbers of chloride ions across the ARA membrane versus acid concentrations [6]. Using increasing acid concentrations, Lorrain *et al*. found a linear increase for the apparent proton transport number in an ARA membrane [14]. It can be concluded that increasing acid concentration induces a linearly increasing proton leakage and a linearly decreasing current efficiency. Consequently, high concentrations were difficult to reach with satisfactory current efficiency. This limiting effect can be attributed to the nonideal selectivity of the two AEM which decreases with increasing HCl concentrations.

In the salt compartment sodium ions are in competition with protons coming from the HCl compartment to cross over the CEM. When protons enter the catholyte compartment, they neutralize hydroxide ions from the cathode to form water molecules. This neutralization contributes to the decreasing current efficiency in sodium hydroxide production. During this neutralization process, the linearly increasing apparent proton transport number also induces a linearly decreasing current efficiency for NaOH.

3.3. *Influence of current density on EED efficiency*

To evaluate the influence of the current density on the EED efficiency, HCl and NaOH were regenerated from solutions of 0.1 M initial concentration and

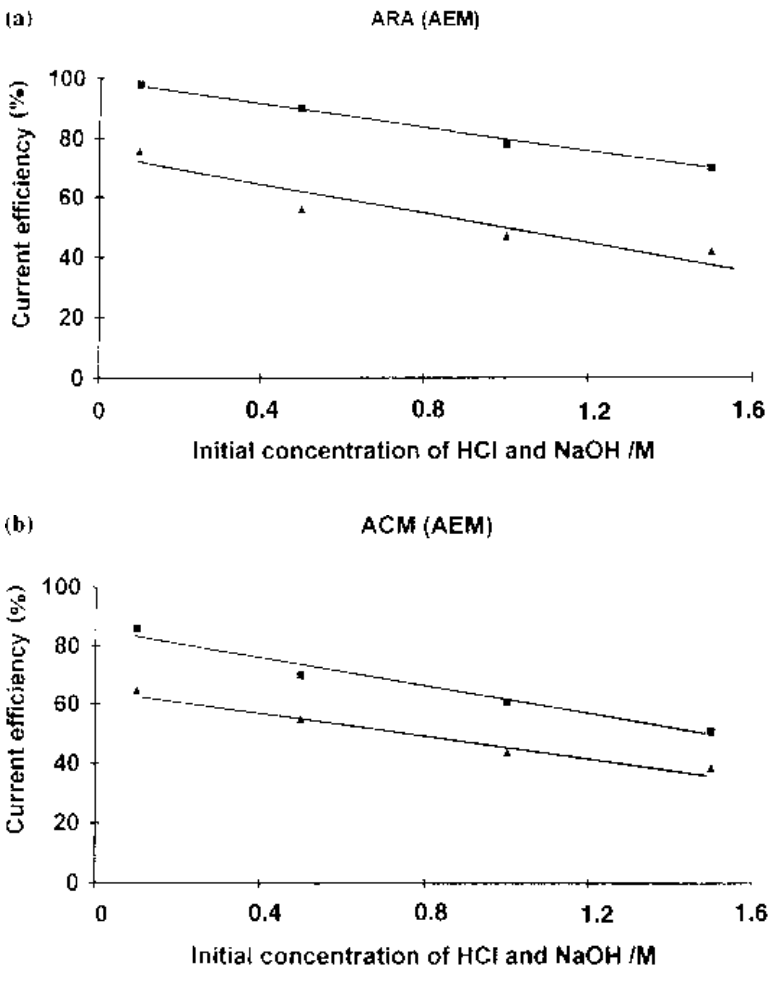

Fig. 3. Current efficiency against initial concentration of HCl (■) and NaOH (▲) at $I = 40\,mA\,cm^{-2}$.

0.5 M NaCl by using three current densities: 40, 80 and 120 mA cm^{-2}. All experiments were performed for 120 min. Figure 4(a) and (b) give for each AEM current efficiencies against current density.

The hydrochloric acid production is generally higher than that of sodium hydroxide production. This difference can be explained by proton leakage through the AEM. After crossing the CEM protons neutralize hydroxide ions at high sodium hydroxide and hydrochloric acid concentrations. Hydroxide ion leakage through the CEM must be added to this phenomenon to explain this difference.

In this experimental range of current densities, current efficiency follows a linear decrease. As in the case of Fig. 3(a) and (b), increasing current densities induces increasing concentration, consequently a linear increase of proton leakage and a linearly decreasing current efficiency result. The highest current efficiencies for the whole range of current densities were obtained with the ARA membrane.

3.4. *Membrane sorption for different electrolytes*

Figure 5 gives the number of sorbed molecules for every site in the ARA, ACM and CMV membranes after equilibrating in different HCl solutions for the AEM and in NaOH solutions for the CMV. This figure shows that at high concentrations, the ACM sorbs more ions than the ARA membrane. In contrast to the NaCl solutions there is no Donnan exclusion at low concentrations with the HCl or NaOH solutions [15, 16]. Table 4 gives the number of sorbed molecules per fixed site for the AEM and CEM when equilibrated in 0.5 M NaCl.

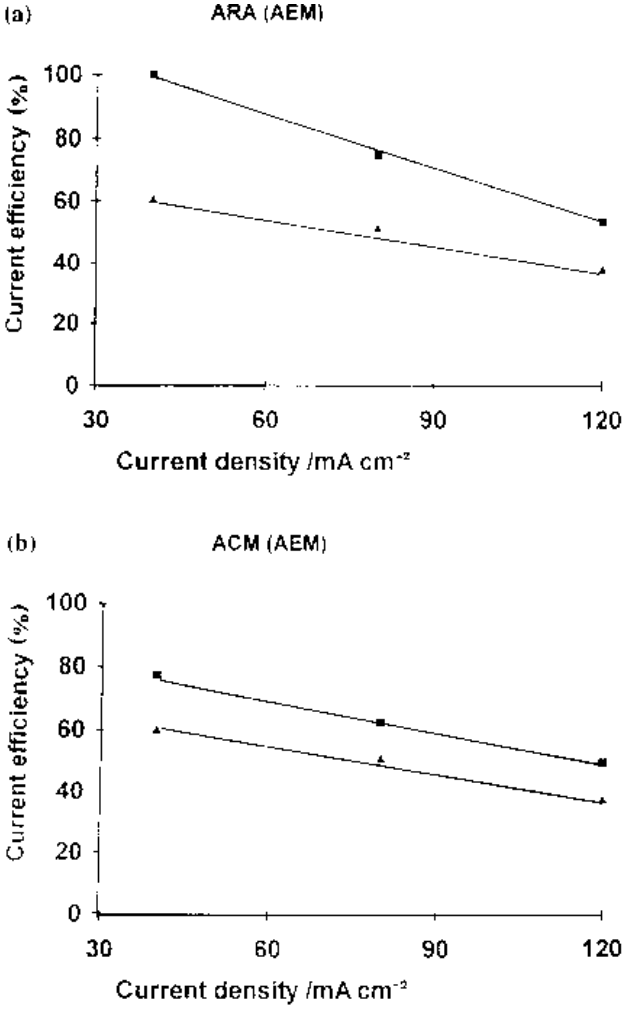

Fig. 4. Influence of current density on current efficiencies at constant initial concentrations (0.1 M). Key: (■) HCl and (▲) NaOH.

3.5. *Determination of diffusion coefficient $\overline{D}_{Cl^-}$ and diffusion coefficients ratios $\overline{D}_{Cl^-}/\overline{D}_{H^+}$ in the AEM*

From the conductance curves in Fig. 6 it is possible to deduce the specific conductivity value λ [17], then the equivalent conductivity λ_e and the conventional mobility $\overline{U}$ through the equation:

$$\lambda_e = \frac{\lambda}{\left[\overline{X}^+\right]} = F\overline{U} \tag{2}$$

where F is the Faraday constant and $\left[\overline{X}^+\right]$ the exchange capacity of the membrane considered as concentration per unit volume. The absolute mobility ($\overline{U}_{abs}$) is a function of the conventional mobility in the CGS unit system through the following relation:

$$\overline{U}_{abs} = 300\frac{1}{z_i e_0}\overline{U} = \frac{300}{z_i e_0}\frac{\lambda}{\left[\overline{X}^+\right]F} \tag{3}$$

where z_i is the charge of the i ion and e_0 the charge of the electron expressed in CGS units. The Nernst–Einstein equation gives the relation between the diffusion coefficient and its absolute mobility:

$$\overline{D}_i = kT\overline{U}_{abs} \tag{4}$$

and, for chloride ions:

$$\overline{D}_{Cl^-} = kT\frac{300}{z_i e_0}\frac{\lambda}{\left[\overline{X}^+\right]F} \tag{5}$$

where k is the Boltzmann constant and T the temperature in kelvin.

From the slopes and the intercepts of the conductance straight lines, the proton to chloride mobility ratio can be determined according to the following series of relations.

Assuming that the membrane volume remains constant with increasing concentration:

$$\Lambda = K(\overline{U}^+\overline{n}^+ + \overline{U}^-\overline{n}^-) \tag{6}$$

The total number of chloride ions per site is equal to the sum of sorbed molecules per site ($\overline{n}_s$) plus one mole to equilibriate the positive fixed site

Table 4. Amount of sorbed molecules per fixed site in the three membranes in 0.5 M NaCl

Membrane	*ARA*	*ACM*	*CMV*
Number of NaCl sorbed moles per site	0.12	0.05	0.069

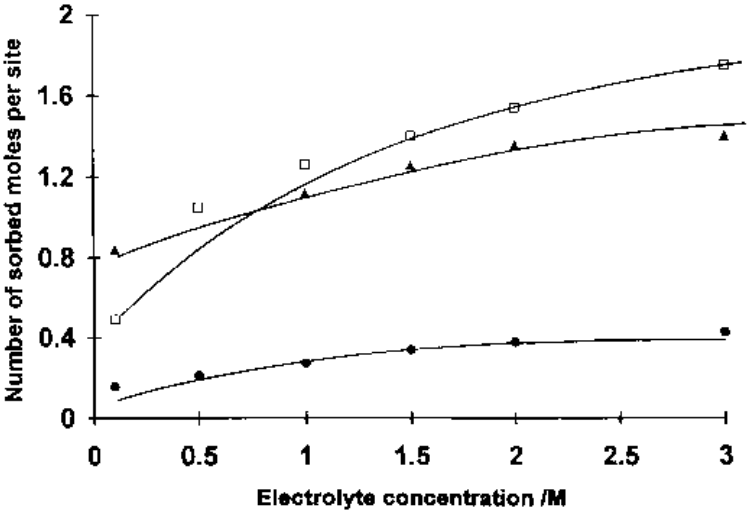

Fig. 5. Amount of sorbed molecules per fixed site against external concentrations of electrolyte (HCl for AEM and NaOH for CEM). Key: (▲) ARA, (□) ACM and (●) CMV.

$$\overline{n}^- = \overline{n}_s + 1 \quad \text{with } \overline{n}_s = \overline{n}^+$$

Equation 6 then becomes

$$\Lambda = K\overline{U}^- + K(\overline{U}^+ + \overline{U}^-)n_s \qquad (7)$$

The experimental straight lines in Fig. 6 are in agreement with this equation if the ionic mobilities inside the membranes are constant. As Λ is a linear function of $\overline{n}_s$ we can determine the ratio of the slope $[b = K(\overline{U}^+ + \overline{U}^-)]$ over the intercept $[a = K\overline{U}^-]$ using the following relation:

$$\frac{b}{a} = 1 + \frac{\overline{U}^+}{\overline{U}^-} = 1 + \frac{\overline{D}^+}{\overline{D}^-} \qquad (8)$$

Thus, it is possible, from chloride diffusion coefficient values inside the membrane and the value of the *b/a* ratio, to determine the ratio of chloride over proton diffusion coefficients and, consequently, the proton diffusion coefficient inside the membrane (Table 5). These results can be used with the Nernst–Planck equations to calculate the relation between flux J_{Cl^-} and the diffusion coefficients.

3.6. *Determination of sodium ion diffusion coefficients and of the sodium to hydroxide diffusion coefficient ratio in the CEM membrane*

As Λ is also a linear function of $\overline{n}_s$, (Fig. 6), the same type of calculation was carried out for this membrane to obtain the diffusion coefficient of the sodium ion:

$$\overline{D}_{Na^+} = 10.54 \times 10^{-7}\ \text{cm}^2\ \text{s}^{-1}$$

and the sodium ion over hydroxide ion diffusion coefficients ratios:

$$\overline{D}_{Na^+}/\overline{D}_{OH^-} = 0.106$$

3.7. *Nernst–Planck equations applied to transport process*

Under the experimental conditions of the exchange flux measurements the diffusion process is mainly controlled by the membrane and the diffusion layer was neglected as a first approximation. The flux of protons (J_{H^+}) and the flux of chloride ions (J_{Cl^-})

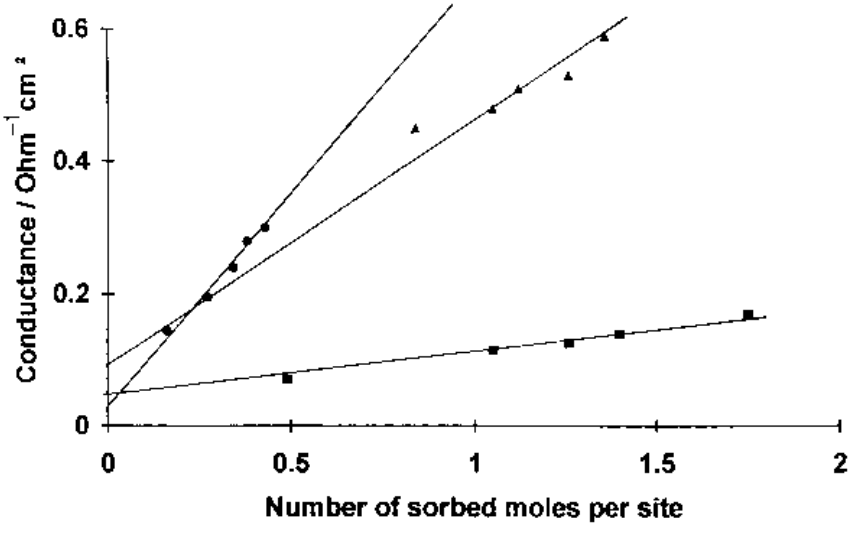

Fig. 6. Conductance variations against the number of sorbed molecules per fixed site. Key: (■) ACM, (●) CMV and (▲) ARA.

Table 5. Chloride diffusion coefficients and chloride over proton diffusion coefficients ratio in AEM

AEM	*ARA*	*ACM*
$10^7 D_{Cl^-}/cm^2 s^{-1}$	4.18	1.03
D_{Cl^-}/D_{H^+}	0.416	0.60

through an anion exchange membrane are given by the two Nernst–Planck equations:

$$J_{H^+} = -\overline{D}_{H^+}\frac{d\left[\overline{H}^+\right]}{dx} - \overline{D}_{H^+}\left[\overline{H}^+\right] f\frac{d\overline{\Phi}}{dx} \qquad (9)$$

$$J_{Cl^-} = -\overline{D}_{Cl^-}\frac{d\left[\overline{Cl}^-\right]}{dx} + \overline{D}_{Cl^-}\left[\overline{Cl}^-\right] f\frac{d\overline{\phi}}{dx} \qquad (10)$$

in which $\left[\overline{H}^+\right]$ and $\left[\overline{Cl}^-\right]$ are the concentrations of the respective ions inside the membrane, and x is the distance through the membrane (Fig. 7). It is assumed that the flux of Na^+ through the AEM may be neglected because of its permselectivity.

The concentration of positive exchange sites, the sorbed protons and sodium ions are equilibrated by negatively charged chloride counter ions:

$$\left[\overline{X}^+\right] + \left[\overline{H}^+\right] + \left[\overline{Na}^+\right] = \left[\overline{Cl}^-\right] \qquad (11)$$

In the present experimental conditions, the concentration of sorbed Na^+ can be neglected compared to protons and fixed site concentrations. The charge of sorbed chlorides is equilibrated by the charge of the sorbed protons.

By combining Equations 9, 10 and 11, integrating the resulting relation and taking into account that the current density is related to the proton and chloride fluxes by

$$I = F(J_{H^+} - J_{Cl^-}) \qquad (12)$$

the following equation is obtained:

$$-J_{Cl^-} = \frac{-2\overline{D}_{Cl^-}}{d(1+\overline{D}_{Cl^-}/\overline{D}_{H^+})}\left(\left[\overline{Cl}^-\right]^0 - \left[\overline{Cl}^-\right]^d\right) + \frac{\overline{D}_{Cl^-}\left[\overline{X}^+\right]}{d(1+\overline{D}_{Cl^-}/\overline{D}_{H^+})} f\left(\overline{\Phi}_0 - \overline{\Phi}_d\right) + \frac{\overline{D}_{Cl^-}/\overline{D}_{H^+}}{1+\overline{D}_{Cl^-}/\overline{D}_{H^+}}\frac{I}{F} \qquad (13)$$

This equation shows that the main factors acting on HCl flux are: (i) the sorbed quantities of chloride ions, which are related to the solution concentrations on each side of the membrane; (ii) the potential difference between the two faces of the membrane. This parameter also depends on the solution concentrations and the structure of the membrane; (iii) the ratio of chloride to proton diffusion coefficients; (iv) the membrane thickness (d); and (v) the current density.

Fig. 7. Membrane system diagram.

3.8. *Diffusion potential in an anion exchange membrane*

From Equations 9–12, the potential difference is obtained:

$$\overline{\Phi}_0 - \overline{\Phi}_d = -I\int_0^d \frac{dx}{fF\left[\overline{D}_{H^+}\left[\overline{H}^+\right] + \overline{D}_{Cl^-}\left(\left[\overline{X}^+\right] + \left[\overline{H}^+\right]\right)\right]} + \int_{\bar{c}_s(x=0)}^{\bar{c}_s(x=d)} \frac{\left(\overline{D}_{Cl^-} - \overline{D}_{H^+}\right)d\left[\overline{H}^+\right]}{\left[\overline{D}_{H^+}\left[\overline{H}^+\right] + \overline{D}_{Cl^-}\left(\left[\overline{X}^+\right] + \left[\overline{H}^+\right]\right)\right]} \qquad (14)$$

By analogy:

$$\overline{\Phi}_0 - \overline{\Phi}_d = IR_M + E_D \qquad (15)$$

The first term is the potential difference due to Ohm's law and the second is the diffusion potential [19].

Integrating this second integral gives:

$$E_D = \frac{1-\overline{D}_{Cl^-}/\overline{D}_{H^+}}{1+\overline{D}_{Cl^-}/\overline{D}_{H^+}}\frac{RT}{F} \ln\frac{\left[\left(1+\overline{D}_{Cl^-}/\overline{D}_{H^+}\right)\left[\overline{H}^+\right] + \left(\overline{D}_{Cl^-}/\overline{D}_{H^+}\right)\left[\overline{X}^+\right]\right]_{x=d}}{\left[\left(1+\overline{D}_{Cl^-}/\overline{D}_{H^+}\right)\left[\overline{H}^+\right] + \left(\overline{D}_{Cl^-}/\overline{D}_{H^+}\left[\overline{X}^+\right]\right)\right]_{x=0}} \qquad (16)$$

Table 6 gives the calculated values of the diffusion potential for the three membranes. Equations 13–16 allow determination of the transfer flux of Cl^- through the membrane when an electric field is applied. The experimental flux (J_{exp}) of chloride ions is obtained during the steady state from the following relation:

$$J_{exp} = \Delta M/At \qquad (17)$$

where ΔM is the number of transferred molecules, A is the active area of the membrane and t is the time of the steady state (30 min during which all measurements were performed). During this time, concentrations increase linearly in compartments I and III and ion fluxes through the membranes remain constant.

Applying the Nernst–Planck equations to this process allows calculation of J_{Cl^-} and J_{H^+} and to compare these values with the experimental results. Initial experimental flux and calculated results of the initial flux are given in Fig. 8(a) and (b). The experimental values are always higher than the calcu-

Table 6. Diffusion potentials against HCl concentrations in the systems: NaCl (0.5 M)/ARA or ACM/HCl (x M) and NaCl (0.5 M)/CMV/NaOH (x M)

HCl or NaOH/M	*0.1*	*0.5*	*1*	*1.5*
ARA/mV	−11.23	−12.45	−13.02	−13.92
ACM/mV	− 4.7	− 7.63	− 8.72	− 9.2
CMV/mV	−20.26	−16.33	−13.05	−9.43

lated ones and undergo the same type of decrease. The gaps between these two curves can be explained in the following terms: (i) the membranes are homogeneous gels; (ii) the diffusion coefficients are constant in the membrane; (iii) the activity coefficients are assumed equal to 1 in the membrane; (iv) the electrical resistance of the membrane is equal to the resistance of the membrane equilibrated in the most conductive solution; (v) the Nernst–Planck equation does not take into account the electro-osmosis process; and (vi) the coupling between individual ion flux is expressed by electroneutrality, which itself is an assumption, by neglecting Poisson's law.

3.9. *Nernst–Planck equations applied to cation exchange membranes (CEM)*

Returning to the Nernst–Planck equations and replacing $[H^+]$ and $[Cl^-]$ by $[Na^+]$ and $[OH^-]$, respectively, and following the same calculation process we obtain a similar relation for J_{Na^+} and for the diffusion potential. These equations show that the transference flux of J_{Na^+} depends on the same factors as J_{Cl^-}. Figure 9 gives the experimental and calculated values of J_{Na^+} through the CMV membrane for different initial concentrations of NaOHz. As with HCl and AEM the calculated values are always lower than the experimental ones. The same comments as in the case of AEM also explain the gap between the two sets of results.

3.10. *Application to El Outaya rock salt*

The same EED experiments were performed with natural El Outaya salt. Solutions were filtered to eliminate insoluble components. Table 7 gives the results of the chemical analysis of this salt and Table 8 the compositions of the solutions obtained.

From the initial concentrations of 0.1 M for HCl and NaOH and 58.5 g dm^{-3} for the rock salt, under a current density of 120 mA cm^{-2}, concentrations of about 2 M were reached after 360 min. During this time the ARA gave higher concentrations than the ACM (Table 8). This table shows the high quality of HCl and NaOH solutions. Only 10 ppm of sodium appear in the HCl due to the diffusing Na^+ crossing over the AEM and about 25 ppm of chloride appears in the NaOH due to diffusing Cl^- crossing the CEM. The small percentages of alkaline earth cations did not hinder the production process. However, in the case of industrial production, in order to eliminate all the ions that may precipitate, the solutions should be pretreated [20].

Table 7. Chemical analysis of El Outaya salt

Element	Cl^-	Na^+	Ca^{2+}	Mg^{2+}	K^+	SO_4^{2-}	*Insoluble*
%	59.52	38.70	0.12	0.06	0	0.41	1.49

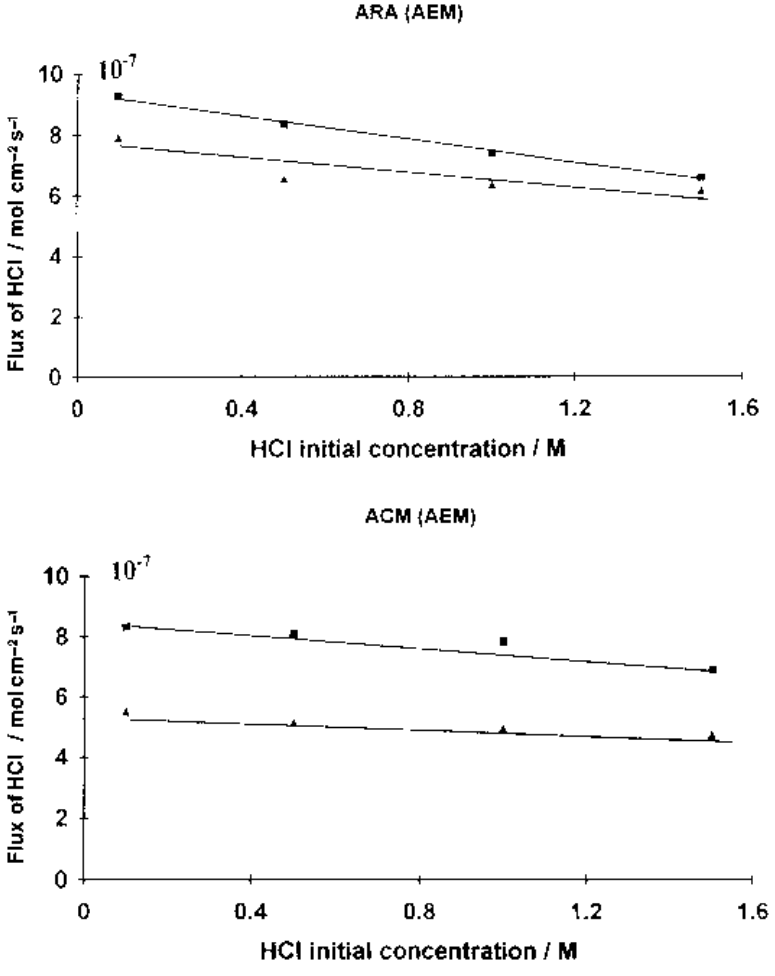

Fig. 8. Calculated (▲) and experimental (■) transfer flux variations of Cl^- or HCl through AEM against HCl initial concentrations. I = 120 mA cm^{-2}.

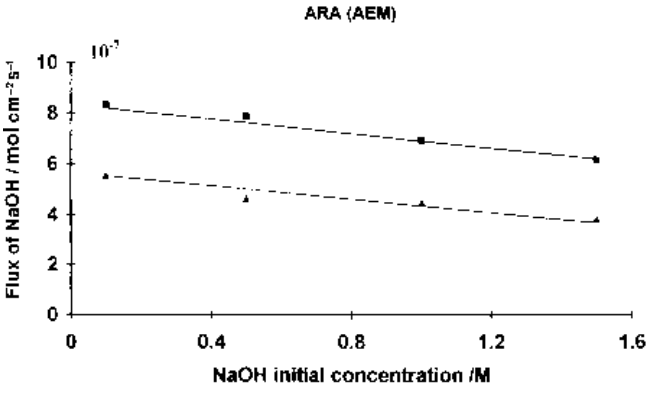

Fig. 9. Calculated (▲) and experimental (■) transfer flux variations of Na^+ or NaOH through CMV against NaOH initial concentrations.

3.11. *Comparing electro-electrodialysis and BPM electrodialysis processes with El Outaya rock salt*

In the same operating conditions as for electro-electrodialysis BPM electrodialysis with a WSI bipolar membrane gives similar HCl and NaOH concentrations. However, the sodium concentration in the acid solution and chloride in the hydroxide solution are greater (Tables 8 and 9). These increasing concentrations can be attributed to the Na^+ and Cl^- leaks through the BPM.

Although BPM electrodialysis permits the use of a stack of cells between two electrodes and larger volumes to be treated, compared to EED for which every cell necessitates a pair of electrodes, final products are somewhat lower in quality because of ion leakage through the BPM.

3.12. *Higher performance cells*

With the laboratory cell satisfactory current efficiencies were obtained. Although the highest current efficiencies were not our main purpose, better performance could be reached with these AEM membranes when used in other types of industrial cells. When the membranes are in a stack system they are separated by grid spacers and the diffusion layer thickness is smaller compared to the laboratory cell, in which the membranes are 10 mm apart. Turbulent flow takes the place of a quasilaminar flow. Because of this smaller thickness, H^+ ions, which result from AEM proton leakage, enter the NaCl compartment at a lower concentration. As the kinetics of the process on this side of the membrane are the most significant, a decrease in proton concentration decreases the gradient inside the membrane and, consequently, leads to a decrease in proton flux (i.e., a decreasing proton leakage). However, this explanation also holds for chloride ions.

Let us consider the transport numbers inside the membrane:

$$\bar{t}_{Cl^-} = \frac{\overline{D}_{Cl^-}\left[\overline{Cl}^-\right]}{\overline{D}_{Cl^-}\left[\overline{Cl}^-\right] + \overline{D}_{H^+}\left[\overline{H}^+\right]} = \frac{\left[\overline{Cl}^-\right]}{\left[\overline{Cl}^-\right] + \frac{\overline{D}_{H^+}}{\overline{D}_{Cl^-}}\left[\overline{H}^+\right]} \tag{18}$$

$$\bar{t}_{H^+} = \frac{\overline{D}_{H^+}\left[\overline{H}^+\right]}{\overline{D}_{Cl^-}\left[\overline{Cl}^-\right] + \overline{D}_{H^+}\left[\overline{H}^+\right]} = \frac{\left[\overline{H}^+\right]}{\frac{\overline{D}_{Cl^-}}{\overline{D}_{H}^+}\left[\overline{Cl}^-\right] + \left[\overline{H}^+\right]} \tag{19}$$

Table 8. Composition of the obtained acid and base with EED process

Membrane	*Product*	Cl^- /mg dm^{-3}	Na^+ /mg dm^{-3}	K^+ /mg dm^{-3}	Ca^{2+} /mg dm^{-3}	Mg^{2+} /mg dm^{-3}	SO_4^{2-} /mg dm^{-3}
ARA	HCl (2.16 M)	77000	10	0	0	0	2
	NaOH (2 M)	28	46000	0	0	0	0
ACM	HCl (2 M)	71000	10	0	0	0	2
	NaOH (1.6 M)	22	36800	0	0	0	0

Table 9. Composition of the obtained acid and base with ED using a BPM membrane

Membrane	*Product*	Cl^- /mg dm^{-3}	Na^+ /mg dm^{-3}	K^+ /mg dm^{-3}	Ca^{2+} /mg dm^{-3}	Mg^{2+} /mg dm^{-3}	SO_4^{2-} /mg dm^{-3}
ARA	HCl(2.06 M)	73130	16	0	0	0	2.5
	NaOH (1.96 M)	30	45080	0	0	0	0
ACM	HCl (1.93 M)	72065	15	0	0	0	2
	NaOH (1.88 M)	37.5	43240	0	0	0	0

Taking for the $\overline{D}_{Cl^-}/\overline{D}_{H^+}$ ratio the average value of 0.5 then

$$\bar{t}_{Cl^-} = \frac{\left[\overline{Cl}^-\right]}{\left[\overline{Cl}^-\right] + 2\left[\overline{H}^+\right]} \quad (20)$$

and

$$t_{H^+} = \frac{\left[\overline{H}^+\right]}{0.5\left[\overline{Cl}^-\right] + \left[\overline{H}^+\right]} \quad (21)$$

Taking into account Equation 11 and assuming as previously that inside the interstitial solution, sodium ion concentration can be neglected, between $\left[\overline{Cl}^-\right]$ and $\left[\overline{H}^+\right]$ the following relation holds:

$$\left[\overline{Cl}^-\right] = \left[\overline{X}^+\right] + \left[\overline{H}^+\right] \quad (22)$$

Equations 20 and 21 become:

$$\bar{t}_{Cl^-} = \frac{\left[\overline{X}^+\right] + \left[\overline{H}^+\right]}{\left[\overline{X}^+\right] + 3\left[\overline{H}^+\right]} \quad (23)$$

and

$$\bar{t}_{H^+} = \frac{\left[\overline{H}^+\right]}{0.5\left[\overline{X}^+\right] + 1.5\left[\overline{H}^+\right]} \quad (24)$$

Differentiating gives:

$$\Delta\bar{t}_{Cl^-} = \frac{-2\left[\overline{X}^+\right]\Delta\left[\overline{H}^+\right]}{\left(\left[\overline{X}^+\right] + 3\left[\overline{H}^+\right]\right)^2} \quad (25)$$

and

$$\Delta\bar{t}_{H^+} = \frac{0.5\left[\overline{X}^+\right]\Delta\left[\overline{H}^+\right]}{\left(0.5\left[\overline{X}^+\right] + 1.5\left[\overline{H}^+\right]\right)^2} \quad (26)$$

This final pair of equations show that with decreasing proton concentration $-\Delta\left[\overline{H}^+\right]$ at the surface of the membrane in contact with the NaCl solution, decreasing $\Delta\bar{t}_{H^+}$ and increasing $\Delta\bar{t}_{Cl^-}$ are obtained. Consequently, electro-electrodialysis using membranes separated by grids gives higher current efficiencies than for laboratory cells. Moreover, with grid separators the compartment thickness being reduced from 10 to 1 mm, the resistance of the cell, the applied voltage and the energy consumption will be greatly decreased.

4. Conclusion

This work shows that it is possible to produce simultaneously HCl and NaOH in safer environmental conditions than with diaphragm or mercury cathode processes. The main limit of this process is proton leakage. The ACM membrane showed lower current efficiencies than the ARA. Applying this process to Algerian rock salt from El Outaya, and using a laboratory cell, satisfactory results were obtained with a current efficiency of 60–70% and products with purity higher than 99.9%.

With these current efficiencies, the concentration of HCl and NaOH was limited to a maximum of 2 M because of the fall in permselectivity of the membranes at high acid or base concentrations. This technique is not limited to classical substitution processes but can also be applied to effluent treatment. Similar results were obtained with BPM electrodialysis. However, sodium concentration in the acid solution and chloride in the hydroxide solution are slightly greater than with EED but also give a purity higher than 99.9%.

It is possible to envisage industrial use of these anion exchange membranes with adapted industrial cells in which membranes are separated by grid spacers in order to reach higher current efficiencies. These membranes can be useful to recycle salts when base and acid at average concentrations are needed.

Acknowledgements

The authors wish to thank Viktor Nikonenko and Thomas Barman for helpful discussions.

References

[1] J. Fauvarque, *Inf. Chimie.* **366** (1995) 91–126.
[2] G. Milazzo, 'Electrochimie', tome 2, 'Applications Industrielles', Dunod, Paris (1969).
[3] I. F. White and T. F. O'Brien, *Mod. Chlor. Alkali Technol.* **4** (1990) 271–89.
[4] A. T. Cherif, C. Gavach, T. Cohen, P. Dagard, and L. Albert, *Hydrometallurgy* **21** (1988) 191–201.
[5] A. T. Cherif and C. Gavach, *J. Electroanal. Chem.* **265** (1989) 143–57.
[6] C. Gavach, T. Cherif, C. Herbert and A. Elmidaoui, 'New Anion Exchange Membranes for Acid Recovery', 5th World Filtration Congress, vol. 1, Nice (1990), p. 429.
[7] A. Elmidaoui, A. T. Chérif, J. Brunéa, F. Duclert, T. Cohen and C. Gavach, *J. Membrane Sci.* **67** (1992) 263–71.
[8] K. M. Mani, F. P. Chandla and C. H. Bysewsky, *Desalination* **68** (1988) 149–66.
[9] D. Raucq, G. Pourcelly and C. Gavach, *ibid.* **91** (1993) 163–75.
[10] R. Simons, *J. Membrane Sci.* **78** (1993) 13–23.
[11] B. Auclair, Private Communication, 'Club Membrane', EDF (1985).
[12] T. Cohen, P. Dagard, J. Molénat, B. Brun and C. Gavach, *J. Electroanal. Chem.* **210** (1986) 329–36.
[13] A. Lindheimer, J. Molénat, and C. Gavach, *ibid.* **216** (1987) 71–88.
[14] Y. Lorrain, G. Pourcelly and C. Gavach, *J. Membrane Sci.* **110** (1996) 181–90.
[15] A. Elmidaoui, A.T. Cherif, J. Molénat, C. Gavach, *Desalination* **101** (1995) 39–46.
[16] A. Oikonomou, Etude du transport de matière dans les membranes ioniques perfluorées en relation avec les propriétés physico-chimiques due matriau, Thèse, Université libre de Bruxelles, Faculté des Sciences (1989).
[17] G. Pourcelly and C. Gavach, *J. Electroanal. Chem.* **259** (1989) 113–25.
[18] F. Helfferich, 'Ion Exchange', McGraw-Hill, New York (1962).
[19] M. Lakshminarayanaiah, 'Transport Phenomena in Membranes', Academic Press, London (1963).
[20] F. Delmas, 'Communication Thématique, Journées d'Electrochimie de Grenoble', (1993).